

QIZHENG GU

RF SYSTEM DESIGN OF TRANSCEIVERS FOR WIRELESS COMMUNICATIONS

 Springer

RF SYSTEM DESIGN OF TRANSCEIVERS FOR WIRELESS COMMUNICATIONS

Qizheng Gu

Nokia Mobile Phones, Inc.

 Springer

Gu, Qizheng, 1936-

RF system design of transceivers for wireless communications / Qizheng Gu.

p. cm.

Includes bibliographical references and index.

ISBN 0-387-24161-2 (alk. paper) -- ISBN 0-387-24162-0 (e-book)

1. Radio--Transmitter-receivers. 2. Wireless communication systems--Equipment and supplies. I. Title.

TK6560.G78 2005

621.384'131--dc22

2005049760

ISBN 0-387-24161-2 e-ISBN 0-387-24162-0 Printed on acid-free paper.
ISBN 978-0387-24161-6

© 2005 Springer Science+Business Media, Inc.

All rights reserved. This work may not be translated or copied in whole or in part without the written permission of the publisher (Springer Science+Business Media, Inc., 233 Spring Street, New York, NY 10013, USA), except for brief excerpts in connection with reviews or scholarly analysis. Use in connection with any form of information storage and retrieval, electronic adaptation, computer software, or by similar or dissimilar methodology now known or hereafter developed is forbidden.

The use in this publication of trade names, trademarks, service marks and similar terms, even if they are not identified as such, is not to be taken as an expression of opinion as to whether or not they are subject to proprietary rights.

Printed in the United States of America.

9 8 7 6 5 4 3 2 1

SPIN 11049357

springeronline.com

Source information, either voice or data, is usually a base-band low-pass signal from DC to a few megahertz. To transmit information in a wireless digital communication system, the base-band signal must be transformed into digital symbols, the symbols are then converted to digital waveforms, and finally the digital waveforms modulate an RF carrier for transmitting. In the receiver chain, a reverse conversion and transformation process is carried out to finally detect received messages.

We discuss sampling theorem, quantization effects, pulse shaping, intersymbol interference, detection error probability, and signal-to-noise ratio or carrier-to-noise ratio.

2.4.1. Sampling Theorem and Sampling Process

In digital communication systems, the analog information must first be transformed into a digital format. The transform process starts with the *sampling process*. This process can be implemented by means of sampling and holding operations. The output of the sampling process is a sequence of pulses with amplitudes derived from the input waveform samples. The following discussion on the sampling process uses an intuitive approach similar to that presented in reference [10].

A band-limited signal without spectral component beyond frequency f_{max} can be completely reconstructed from a set of uniformly spaced discrete-time samples if the samples are obtained with a sampling rate f_s ,

$$f_s \geq 2f_{max} . \quad (2.4.1)$$

This particular statement is known as the *uniform sampling theorem*. The sampling rate $f_s = 2f_{max}$ is also referred as the *Nyquist rate*.

Assume that an analog waveform $x(t)$ with a Fourier transform $X(f)$, which is equal to zero, while $|f| \geq f_{max}$ as shown in Fig. 2.20(a) and (b).

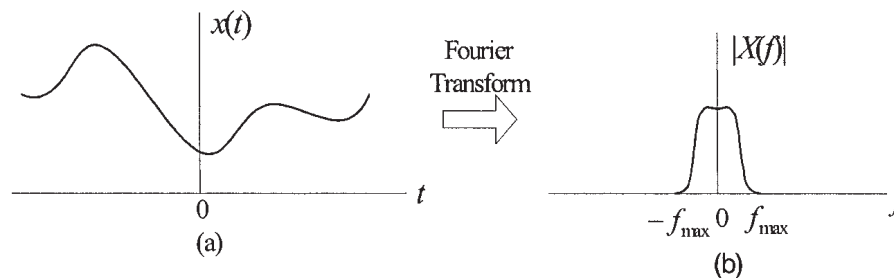


Figure 2.20. Analog waveform (a) with a finite bandwidth spectrum (b)

An *ideal sampling* of $x(t)$ can be viewed as the product of $x(t)$ with a periodic train of impulse functions $x_\delta(t)$, defined as

$$x_\delta(t) = \sum_{n=-\infty}^{\infty} \delta(t - nT_s), \quad (2.4.2)$$

where $T_s = 1/f_s$ is the sampling period and $\delta(t)$ is the unit impulse or Dirac delta function. The sampled version of $x(t)$ as depicted in Fig. 2.21(a) is denoted as $x_s(t)$ and can be expressed as

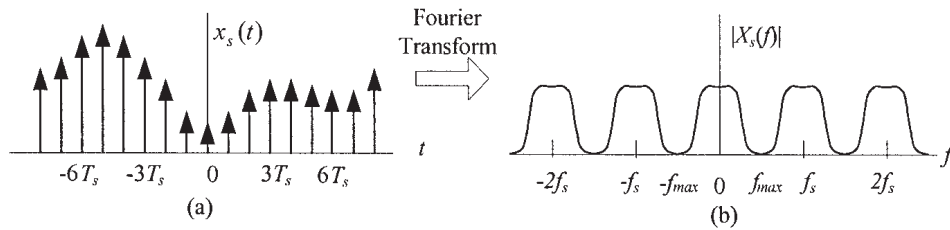


Figure 2.21. Impulse sampled signal and its spectrum

$$x_s(t) = x(t)x_\delta(t) = \sum_{n=-\infty}^{\infty} x(t)\delta(t - nT_s) = \sum_{n=-\infty}^{\infty} x(nT_s)\delta(t - nT_s), \quad (2.4.3)$$

where the following shifting property of the impulse function is used:

$$x(t)\delta(t - t_o) = x(t_o)\delta(t - t_o). \quad (2.4.4)$$

The spectrum of the sampled signal $x_s(t)$ can be obtained from the Fourier transform of (2.4.3). Considering the convolution property of the Fourier transform (see Section 2.1), the Fourier transform of the sampled signal, $X_s(f)$ can be expressed as the convolution of $X(f)$ and the Fourier transform of the impulse train $x_\delta(t)$, $X_\delta(f)$ — i.e.,

$$X_s(f) = X(f) * X_\delta(f) = X(f) * \left[\frac{1}{T} \sum_{n=-\infty}^{\infty} \delta(f - nf_s) \right] = \frac{1}{T} \sum_{n=-\infty}^{\infty} X(f - nf_s), \quad (2.4.5)$$

where the following frequency domain form of the impulse train is used:

$$X_s(f) = \frac{1}{T_s} \sum_{n=-\infty}^{\infty} \delta(f - nf_s). \tag{2.4.6}$$

The spectrum $X_s(f)$ of the sampled signal $x_s(t)$ is, to within a constant factor ($1/T_s$), exactly the same as $X(f)$ of the original signal $x(t)$. In addition, the spectrum repeats itself periodically in frequency every f_s hertz as shown in Fig. 2.21(b).

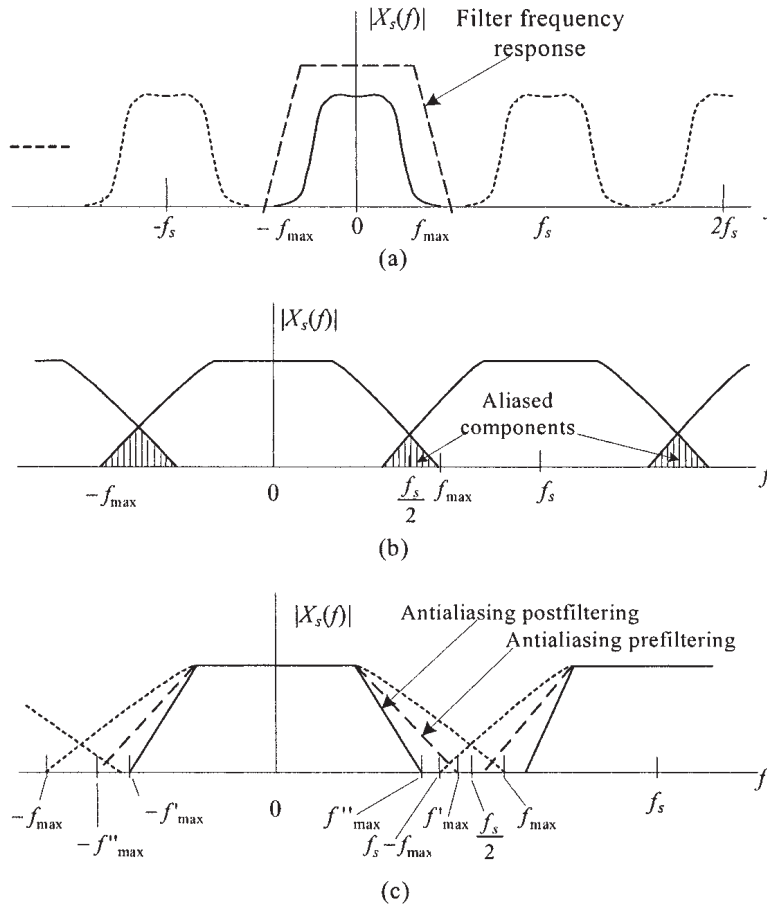


Figure 2.22. Spectra of sampled signals (a) $f_s > 2f_{max}$, (b) $f_s < 2f_{max}$, aliasing components, and (c) eliminating aliasing using antialiasing filters: prefiltering $f'_{max} < f_s/2$ or postfiltering $f''_{max} < f_s - f_{max}$

If the sampling frequency f_s is greater than $2f_{max}$, a low-pass filter can be used to separate the base-band spectrum from the replications at higher frequencies as illustrated in Fig. 2.22(a). When the sampling frequency is less than the Nyquist rate, $f_s < 2f_{max}$ — i.e., in the

undersampling case, the replications will overlap as depicted in Fig. 2.22(b). This spectral overlap of the replications is called *aliasing phenomenon*. Part of the information contained in the original signal will be lost when aliasing occurs. Using antialiasing filters in the undersampling case, we can eliminate the aliasing phenomenon as shown in Fig. 2.22(c). The analog signal is prefiltered so the new maximum frequency f''_{max} is reduced to equal to or less than $f_s/2$. The aliased components can also be removed by postfiltering after sampling; the filter cutoff frequency f''_{max} should be less than $f_s - f_{max}$. However, using antialiasing filters it will still result in a loss of some of the signal information. For an engineering application, it is usually best to choose the lowest sampling rate as

$$f_s \geq 2.2f_{max} . \quad (2.4.7)$$

The instantaneous impulse sampling is a theoretically convenient model. A more practical approach of accomplishing the sampling is to use the rectangular pulse train or switching waveform, $x_p(t)$, as shown in Fig. 2.23(a). Each rectangular pulse in $x_p(t)$ has a width T and an amplitude $1/T$. The Fourier series of the pulse train with a repeated rate f_s has a form

$$x_p(t) = \sum_{n=-\infty}^{\infty} a_n e^{j2\pi n f_s t} , \quad (2.4.8)$$

where a_n is a sinc function in the form

$$a_n = \frac{1}{T_s} \text{sinc}\left(\frac{\pi \cdot nT}{T_s}\right) = \frac{1}{T_s} \frac{\text{Sin}(\pi \cdot nT/T_s)}{\pi \cdot nT/T_s} \quad (2.4.9)$$

and $T_s = 1/f_s$. The magnitude spectrum of the periodic pulse train is given in Fig. 2.23(b), and the envelope of the spectrum has the sinc function shape. The sampled sequence $x_s(t)$ of a band-limited analog signal $x(t)$ (Fig. 2.20(a)) can be expressed as

$$x_s(t) = x(t)x_p(t) = x(t) \sum_{n=-\infty}^{\infty} a_n e^{j2\pi n f_s t} . \quad (2.4.10)$$

This kind of sampling is referred to as *natural sampling*, since the top of each pulse in $x_s(t)$ retains the same shape of its corresponding analog

waveform segment in the pulse interval as illustrated in Fig. 2.23(c). The Fourier transform $X_s(f)$ of the sampled signal is as follows:

$$X_s(f) = F \left\{ x(t) \sum_{n=-\infty}^{\infty} a_n e^{j2\pi n f_s t} \right\} = \sum_{n=-\infty}^{\infty} a_n X(f - f_s). \quad (2.4.11)$$

The spectrum of the natural sampled signal is depicted in Fig. 2.23(d).

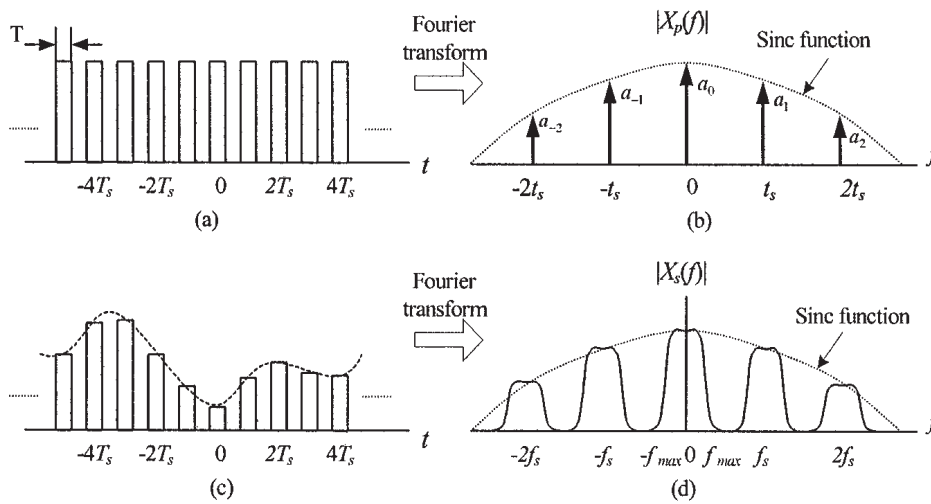


Figure 2.23. Finite pulse sampled signal and its spectrum

In reality, the most popular sampling method is the *sampling and hold*. It can be represented by the convolution of the sampled impulse train (2.4.3), $[x(t)x_\delta(t)]$, with a unity amplitude rectangular pulse $p(t)$ of pulse width T_s :

$$x_s(t) = p(t) * [x(t)x_\delta(t)] = p(t) * \left[x(t) \sum_{n=-\infty}^{\infty} \delta(t - nT_s) \right]. \quad (2.4.12)$$

This convolution results in a flat-top sampled sequence. Its Fourier transform is the product of the Fourier transform $P(f)$ of the rectangular pulse and the spectrum (2.4.5) of the impulse sampled sequence — i.e.,

$$X_s(f) = P(f) \frac{1}{T_s} \sum_{n=-\infty}^{\infty} X(f - n f_s), \quad (2.4.13)$$

where $P(f) = T_s \text{sinc}(fT_s)$. The spectrum of the sample and hold sequence is similar to that presented in Fig. 2.23(d). The hold operation will significantly attenuate the high-frequency replicates. Usually postfiltering is necessary to further suppress the residual spectral components of the replicates at the multiples of the sampling frequency.

A typical sample and hold circuit is shown in Fig. 2.24. In this circuit, the sampled analog voltage is held on capacitor C_H during the analog to digital conversion. After the sample and hold circuit, usually an analog-to-digital converter follows.

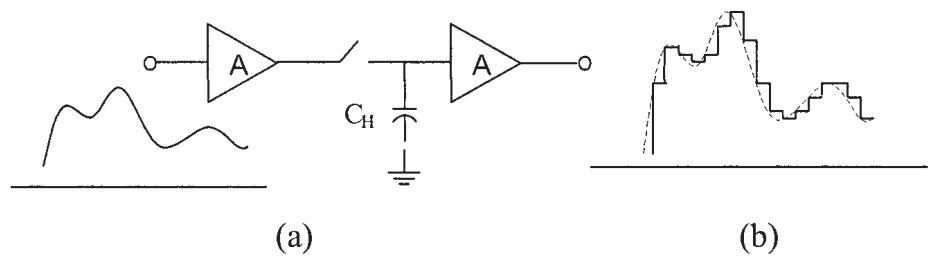


Figure 2. 24. Typical sample and hold circuit (a) and its output (b)

The pulses presented in Fig. 2.23(c) are called quantized samples, and the output waveform of sample and hold circuit is shown in Fig. 2.24(b). These formats can be interfaced with a digital system when the sample values are quantized to a finite set. After quantization, the analog waveform can still be recovered to certain precision, but the reconstruction fidelity can be improved by increasing the number of the quantization level.

2.4.2. Jitter Effect of Sampling and Quantizing Noise

The sampling theorem predicted precise reconstruction of the signal is based on uniformly spaced samples of the signal. The sampling becomes no longer uniform if there is a slight jitter in the position of samples. The jitter is usually a random process, and the position of the samples is not exactly known. The jitter effect is equivalent to FM modulation of the base-band signal. If the jitter is random, noise with a low-level wide-band spectrum is induced. If the jitter appears in a periodic manner, an FM disturbance with low-level discrete spectral lines is generated.

The jitter effect can be measured by means of *signal-to-noise ratio* (SNR). If the input signal is

image rejection. In the low IF receiver with the imbalance compensation, the gain control imbalance in the I and Q two channels may not be so critical since the imbalance can be calibrated and then compensated based on the stored calibration information.

A digital AGC may be needed as in the direct conversion receiver when the LPF or the BPF does not have enough suppression to the blocking and other interferers. More details on the digital AGC can be found in 3.2.3.5.

3.3.3.4. Transmitter with OPLL

The transmitter given in Fig. 3.21 is a superheterodyne GSM transmitter by using offset phase locked loop (OPLL) as a tracking bandpass filter turned to the desired transmission signal. The OPLL used in the GSM transmitter should have the following characteristics: a sufficient suppression level of the transmission noise, a small phase error, and a fast settling. The band-pass characteristic of the OPLL makes it able to replace the transmission SAW and the duplexer. The fast settling can lower the current consumption.

The bandwidth of the OPLL must be narrow enough to suppress noise emission in the receiver band to below -79 dBm, and it must also be broad enough to reproduce the input at the output of the OPLL with a rms phase error less than 5 degree. The optimize bandwidth of the OPLL is in between 0.6 and 2.6 MHz [18].

3.4. Band-pass Sampling Radio Architecture

At present, it is still not practical for mobile stations to use the so-called *software radio* architecture, which should ideally have the ADC placed in the RF front-end near the antenna as possible and operating at an RF sampling frequency slightly higher than twice the greatest carrier frequency of interest, and the resulting samples are processed on a programmable signal processor. For a 1.9 GHz PCS band signal, the sampling rate of the ADC in the ideal software radio should be greater than 4.0 GHz. The main issue here is that the current technology is not mature enough to provide a device of processing samples at such a high rate and with acceptable power consumption for mobile stations. An alternate solution is to use the *band-pass sampling* architecture, which possibly possesses some features of the ideal software radio.

The band-pass sampling also referred to as *harmonic sampling* is the techniques of sampling at rates lower than the highest frequency of interest to achieve frequency conversion from RF to low IF or base-band through *intentional aliasing* and to be able to exactly reconstruct the information content of the sampled analog signal if it is a band-pass signal [19], [20] and [21]. The sampling rate requirement is no longer based on the RF carrier, but rather on the information bandwidth of the signal. Thus the resulting processing rate can be significantly reduced.

The radio architecture will be much simpler than the other architectures presented in the previous sections if the band-pass sampling is directly employed at RF. In this case, the analog RF block contains only band-pass filters and low-noise amplifiers before a high-performance ADC carrying out sampling and digitizing. It should be noticed that the ratio of the RF carrier to the *undersampling* rate used in the band-pass sampling architecture for RF transceivers is usually not high. The main reason for this is due to the noise density of present ADCs operating at RF being high and increasing with the harmonic order of the sampling rate. On the other hand, it is apparent that the band-pass sampling can also be applied in the super-heterodyne receiver to replace the I/Q down-converter and then the BB I and Q channels are created in digital domain. In this section, the RF band-pass sampling will be mainly discussed.

3.4.1. Basics of Band-pass Sampling

The sampling theory shows that, to avoid aliasing and to completely reconstruct the signal, the sampling rate must be at least twice of the highest frequency component in the signal as described in Section 2.4.1. It is implicit that the useful information of signal covers the entire band from zero frequency to cutoff frequency. However, the RF signals used in the wireless communications are usually narrow-band in nature since the signal bandwidths are only 0.003 to 0.2% of their carrier frequencies. In these cases, the minimum uniform sampling rate to avoid aliasing depends on the signal bandwidth instead of the highest frequency of interest. The minimum sampling rate for aliasing-free can be as low as twice of the signal bandwidth if the carrier frequency of the signal is properly chosen. However, the minimum sampling rate $f_{s,min} = 2 \cdot BW$ (where BW is the signal bandwidth) just has its theoretical value in the sense that not only any imperfections in the implementation based on this sampling rate will cause aliasing, but also the band-pass sampling unlike the BB sampling case may still have aliasing problem even if the sampling rate is greater than this $f_{s,min}$.

Assume that a band-pass analog signal has its lowest frequency of interest f_L and the highest frequency of interest f_H or the bandwidth of the signal equals $BW = (f_H - f_L)$. The band-pass analog signal can be exactly reconstructed after sampling and digitizing if the sampling rate f_s meets the following two inequalities [20]:

$$\frac{(n-1)f_s}{2} < f_L \quad (3.4.1)$$

and

$$f_H < \frac{nf_s}{2}, \quad (3.4.2)$$

where n is an integer given by $1 \leq n \leq \lfloor f_H / BW \rfloor$ ($\lfloor \cdot \rfloor$ denotes the largest integer). The sampling rate f_s meeting (3.4.1) and (3.4.2) also means the resulting spectra of the sampled signal have no overlapping or aliasing as clearly shown in Fig. 3.27.

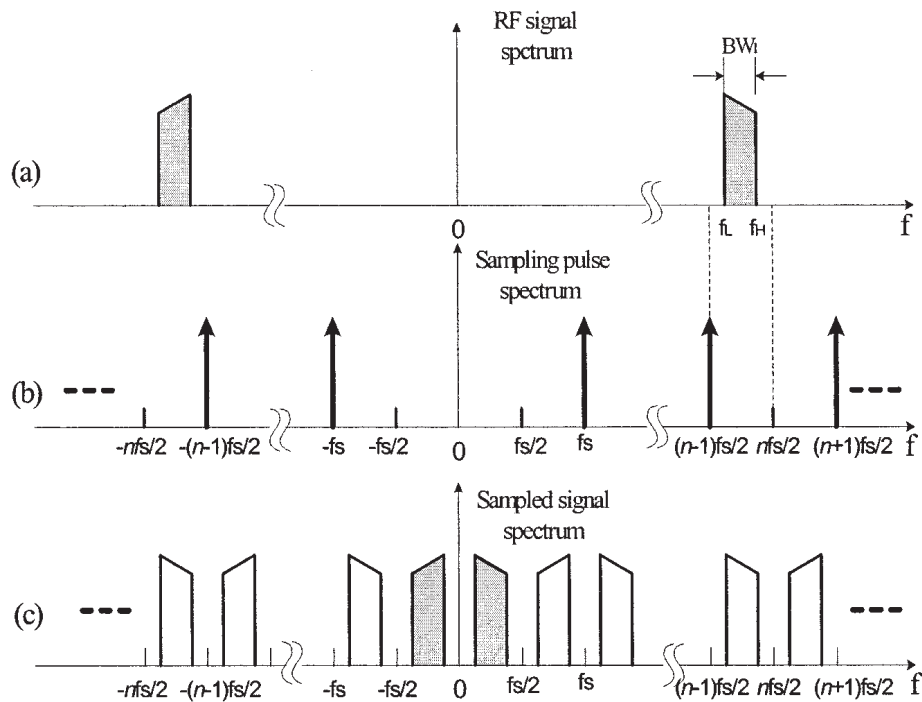


Figure 3.27. Spectra of band-pass sampling: (a) RF signal spectrum, (b) sampling pulse spectrum, and (c) sampled signal spectrum

From inequalities (3.4.1) and (3.4.2) we can determine the acceptable uniform sampling rates for *aliasing-free* to be

$$\frac{2f_H}{n} \leq f_s \leq \frac{2f_L}{n-1}. \quad (3.4.3)$$

The maximum allowable value of n for the band-pass signal with the lowest and highest frequencies f_L and f_H , n_{\max} , is

$$n_{\max} = \left\lfloor \frac{f_H}{f_H - f_L} \right\rfloor. \quad (3.4.4)$$

Equation (3.4.3) can be described graphically as shown in Fig. 3.28 when $n = 1, 2, \dots, 5$. Where the normalized sampling frequency f_s/BW versus the normalized highest frequency f_H/BW is plotted as presented in [19]. The areas inside the wedges are the permissible zones for sampling without aliasing. The shadowed area represents the sampling rates that result in aliasing. It is apparent the aliasing-free ranges of the sampling rate and the highest signal frequency of interest, Δ_s and Δ_{f_H} , increase with normalized sampling rate and the highest signal frequency. The smaller the

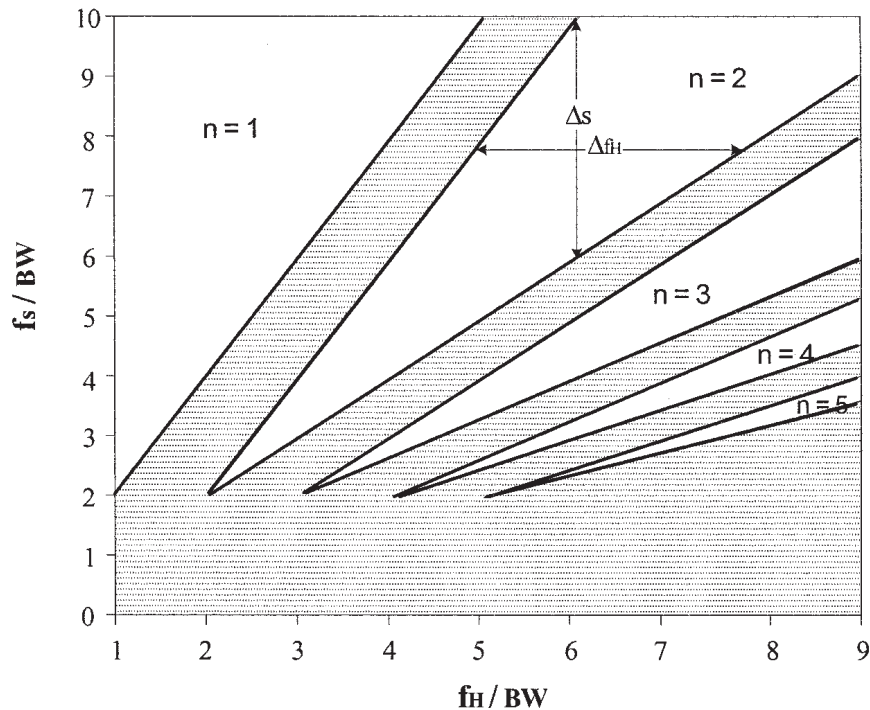


Figure 3.28. Permissible zones for uniform sampling without aliasing

integer number n is, the broader the permissible area for sampling without aliasing will be. The n is usually low less than 10 when the band-pass sampling technique is used for converting an RF signal to a low IF or base-band signal.

In the mobile station applications, it is more practical to consider the signal bandwidth of interest, $BW = (f_H - f_L)$, as the stop bandwidth of the channel filter BW_S and the signal information bandwidth as the pass-band of the channel filter $BW_P = BW_I$, as depicted in Fig. 3.29a. In addition, the center frequency of the pass-band f_c usually represents the carrier frequency of the desired signal. From Fig. 3.29, the frequency difference between the edge of the stop-band bandwidth and the sampling harmonic frequency mf_s nearest to the center frequency f_c , Δ_1 is

$$\Delta_1 = mf_s - (f_c - BW_s/2). \tag{3.4.5}$$

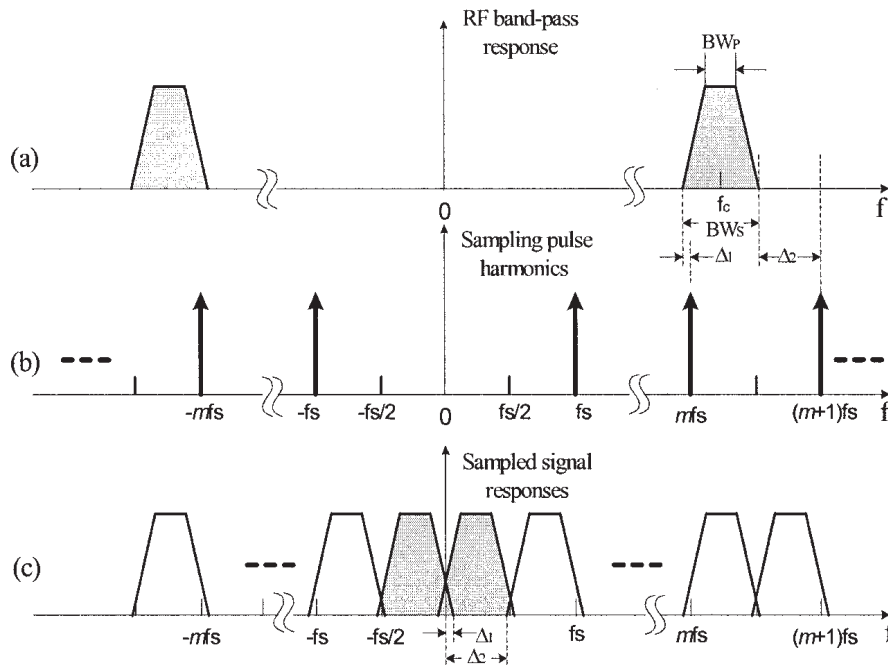


Figure 3.29. RF band-pass response, sampling pulse fundamental and harmonics, and sampled signal responses

The frequency difference between the sampling harmonic $(m+1)f_s$ and another edge of the stop-band bandwidth, Δ_2 is

$$\Delta_2 = (m+1)f_s - (f_c + BW_s/2). \quad (3.4.6)$$

It is apparent from Fig. 3.29(c) that for sampling without aliasing — i.e., no spectrum overlapping into pass-band the Δ_1 and Δ_2 must meet the following inequalities, respectively,

$$\Delta_1 < (f_c - mf_s) - \frac{BW_P}{2} \quad (3.4.7)$$

and

$$\Delta_2 > (f_c - mf_s) + \frac{BW_P}{2}. \quad (3.4.8)$$

Substituting (3.4.5) and (3.4.6) into (3.4.7) and (3.4.8), respectively, the sampling rate without aliasing can be derived as [21]

$$\frac{2f_c + \frac{1}{2}(BW_P + BW_S)}{n} < f_s < \frac{2f_c - \frac{1}{2}(BW_P + BW_S)}{n-1}, \quad (3.4.9)$$

where $n = 2m + 1$. In fact, n in (2.3.9) can be also an even integer or $n = 2m$, and in this case the sampled signal spectrum is inverted [21]. (3.4.9) will turn into (3.4.5) when letting

$$\frac{1}{2}(BW_P + BW_S) = f_H - f_L \quad \text{and} \quad f_c = \frac{f_H + f_L}{2}.$$

The sampling rate precision can be estimated in terms of the difference of the maximum and minimum allowed sampling rates, Δf_s , as follows [19]:

$$\Delta f_s = \frac{2(f_H - BW)}{n-1} - \frac{2f_H}{n}.$$

The relative precision required of the sampling rate is

$$\frac{\Delta f_s}{BW} = \frac{2}{n(n-1)} \left(\frac{f_H}{BW} - n \right) \approx 0 \left(\frac{1}{n^2} \right). \quad (3.4.10)$$

The band-pass sampling relocates the RF band-pass signal to a low-pass position. The resulting signal-to-noise ratio is poorer than that from an analog quadrature down-converter. The signal-to-noise ratio for the sampled

signal SNR_s is degraded by at least the noise aliased from the bands between DC and the RF pass-band, and it becomes

$$SNR_s = \frac{P_S}{P_{N_{in}} + (n-1)P_{N_{out}}}, \quad (3.4.11)$$

where P_S is the spectral power density of the band-pass signal, $P_{N_{in}}$ and $P_{N_{out}}$ are in-band and out-of-band noise power densities, respectively, and n is a positive integer number less than or equal to n_{max} given in (3.4.4). Since there is often a lot of gain in front of the ADC, the in-band noise power density is usually greater than the out-of-band noise power density — i.e., $P_{N_{in}} \gg P_{N_{out}}$ — and thus the SNR_s is mainly determined by $P_S / P_{N_{in}}$. However, if $P_{N_{in}} \cong P_{N_{out}}$ and $n \gg 1$, the degradation of the signal-to-noise ratio in dB can be approximately expressed as

$$D_{SNR} \cong 10 \log(n). \quad (3.4.12)$$

The degradation of the signal-to-noise ratio in the band-pass sampling is caused by the sampling jitter and the quantization noise of the ADC as in the case of BB sampling. The estimation of the SNR_s degradation due to the sampling jitter and the quantization noise can be found in Section 2.4.2.

3.4.2. Configuration of Band-pass Sampling Radio Architecture

A block diagram of the band-pass sampling architecture radio for a full-duplex transceiver, such as a CDMA transceiver, is presented in Fig. 3.30. In this block diagram the receiver and the transmitter both use the harmonic sampling to translate the carrier frequency from an RF to a low IF or vice versa. A proper low IF is needed to avoid the aliasing, and the IF should be low enough for the DSP to handle it. Comparing the band-pass sampling radio with the others, it is apparent that the RF analog block configuration of this radio architecture is much simpler than any one of the architectures presented in the previous sections. The radio architecture based on directly sampling the RF signal is also referred to as digital direct conversion.